2014-EMC-0125.R2 – SUBMISSION 15/07/2014

Application of Fractional Slot-Concentrated Windings to Synchronous Reluctance Motors

C. M. Spargo, *Member, IEEE*, B. C. Mecrow, *Member, IEEE*, J. D. Widmer and C. Morton

***Abstract*—This paper presents an investigation into the application of fractional slot-concentrated windings (FSCW) to synchronous reluctance motors (SynRM). The advantages and disadvantages of the synthesis of such a machine are explored with thermal aspects included and a comparison with a similar topology, the switched reluctance motor (SRM) is also presented where appropriate. The differences in electric drive between the two reluctance motors are briefly explored. Finite element studies show that the fractional slot-concentrated wound machine can exhibit a higher efficiency and torque density when compared to conventional synchronous reluctance and the induction motor and the electromagnetic model is validated through testing of a prototype machine with thermal results also reported. Despite the many benefits, high torque ripple and low power factor reduce the topologies desirability and are identified as an area of further research.**

***Index Terms*— Electric vehicles, Fractional slot concentrated windings, synchronous reluctance, traction motor**

I. Introduction

SYNCHRONOUS reluctance machines (SynRM) are AC synchronous motors that develop only a reluctance torque and were first introduced by Kostko [1] in 1923. As the demand for pure (PEV) and hybrid (HEV) electric vehicles increases, the challenge to design and manufacture high torque density, wide speed range electric motors for these demanding applications is highlighted. Permanent magnet based brushless-DC motors, have been heavily explored, such as those in [2-4]. Induction motor drives have also been considered [5,6] and there has been a recent resurgence in switched reluctance (SRM) technology for future traction applications. The SynRM on the other hand is another alternative and the permanent-magnet assisted SynRM (PMA-SynRM) has raised some interest in this area [7]. However, pure reluctance SynRMs have been neglected. The synchronous reluctance motor has in the literature, consisted solely of polyphase distributed wound stators [8,9,10]. PM based machines and SRM drives typically utilise fractional slot-concentrated windings (FSCW) due to their inherent advantages [11]. Many PM machine designs have been presented [12,13] with one IM being presented [14] and SRM technology having this winding type as a fundamental aspect of their conventional topology [15]. The authors introduce the concept of a fractional slot-concentrated wound synchronous reluctance machine (cSynRM), illustrated alongside a conventional synchronous reluctance motor in Fig. 1. In modern traction drives, for applications such as rail and automotive; factoring in the rare earth challenges the engineering industry faces, reluctance motors are a contender for the future of transportation. Application of FSCWs' to SynRMs in order to synthesise a high performance cSynRM suitable for such applications is the focus of the authors' research. This paper explores the options for such machines and reports upon the key characteristics of the cSynRM in comparison with conventional topologies.

The authors are with the Power Electronics, Machines and Drives Research Group, School of Electrical and Electronic Engineering, Newcastle University, Newcastle-Upon-Tyne, NE1 7RU, UK (e-mail: c.m.spargo@ncl.ac.uk).

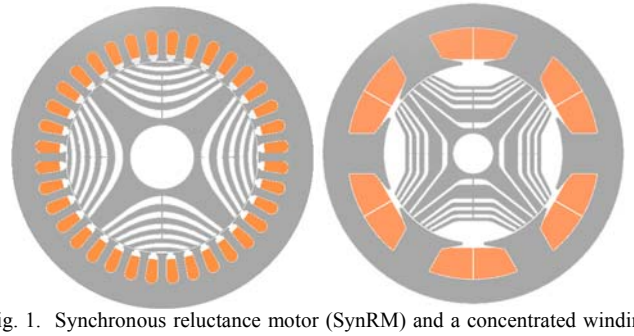

Fig. 1. Synchronous reluctance motor (SynRM) and a concentrated winding synchronous reluctance motor (cSynRM).

II. The Concept

Polyphase distributed windings have long end windings that do not contribute to torque production, only Joule loss and weight. The concept of the new topology is to minimise this, similar to the switched reluctance motor – utilising non-overlapping single tooth wound coils. A comparison of key topology characteristics between the cSynRM (Fig. 1, right) and the SRM is presented in Table. I.

TABLE I
Key Topology Characteristics

	SRM	*cSynRM*
Airgap bore	Doubly salient	Salient stator
Stator coils	Single tooth non-overlapping	
Excitation current	DC pulses	Balanced sinusoidal
Electric Drive	Non-conventional	Conventional
Phase mutual coupling	No	Yes

Therefore the switched reluctance motor and the fractional slot-concentrated wound synchronous reluctance motor have topological similarities, however their excitation and drive requirements are vastly different and are explored further in Section V.

III. Advantages of Single Tooth Coils

For an m phase machine, with n coils per phase, N series turns per phase, with conductor conductivity, σ_e, a RMS stator current, I_s enclosed in a slot of area, A_{slot} and slot fill factor, S_{FF}, the winding loss can be expressed;

$$P_{Cu} = mnI_s^2N^2\left(\frac{l_{\text{ave}}}{\sigma_e A_{slot} S_{FF}}\right) \quad (1)$$

Where, $l_{\text{ave}} = 2L + l$, L is the active conductor length of a coil and l is the end winding length per coil. Thus loss reduction can be achieved by increasing the fill factor or reducing the end turn length if the machine geometry is to remain constant.

A. High Fill Factor

As in the SRM, a higher fill factor can be achieved than in the conventional SynRM, effectively reducing the copper loss in the machine. The copper loss is a function of the slot fill factor $S_{FF} = \frac{A_{Cu}}{A_{Slot}}$ and average turn length l_{ave}, $P_{Cu} \propto \frac{l_{\text{ave}}}{S_{FF}}$. As the coil span is only one tooth, very tight and neat coils can be wound. An increase of fill factor from 30% (a near reasonable value for a distributed winding induction machine based on measurements and experience [37]) to 60% (achievable with bobbin wound coils), reduces the winding loss by 50% (Fig. 2). Therefore there is an immediate advantage to the application of FSCW if high fill can be achieved, being advantageous to machine designers working toward designs for the IE4 Super-Premium efficiency legislation (or NEMA equivalent) or for low loss high torque density traction drives. Slot closures prevent coils being prewound and slid onto the teeth, hence a segmented stator approach can be adopted.

B. Increased Slot Thermal Conductivity

As a direct consequence of the higher fill factor, the amount of air in the slot is significantly reduced and replaced by copper. With the thermal conductivity of air λ_{Air} of $0.029967\text{W}\cdot\text{m}^{-1}\cdot\text{K}^{-1}$ and the relatively high thermal conductivity λ_{Cu} of 390 $\text{W}\cdot\text{m}^{-1}\cdot\text{K}^{-1}$ for copper and increasing the fill factor, the effective slot thermal conductivity can increase significantly. As a first order approximation (neglecting wire insulation and slot liner) of the equivalent slot thermal conductivity can be written [16];

$$\lambda_{\text{eq}} = \lambda_{\text{Air}}\frac{(1+S_{\text{FF}})\lambda_{\text{Cu}} + (1-S_{\text{FF}})\lambda_{\text{Air}}}{(1-S_{\text{FF}})\lambda_{\text{Cu}} + (1+S_{\text{FF}})\lambda_{\text{Air}}} \quad (2)$$

As is evident in Fig. 2, if again the slot fill factor is increased from 30% to 60%, the slot thermal conductivity doubles, effectively halving the winding temperature (assuming equal slot width). Staton [37] presented a linear fit based on measured results on seven induction motors, which is also presented as a comparison (see Appendix B). The cSynRM can be perceived to have a potential thermal advantage over the SynRM and IM. However, if different slot numbers an identical stator bore are compared, the different slot widths are expected to have an effect on the slot thermal conductance. This is explored deeper in Section VII.

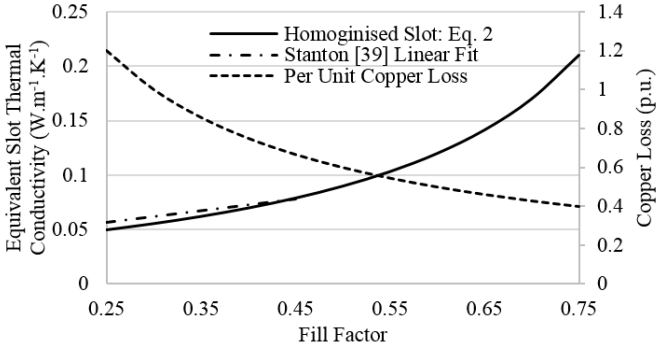

Fig. 2. Per-unit copper loss and effective slot thermal conductivity as a function of slot fill factor, with Staton linear fit.

C. Short End Windings

Switched reluctance machines inherently use single tooth windings and therefore enjoy short end windings, both axially and circumferentially. The circumferential length of end windings can be analytically approximated [17]. In distributed winding machines, the average end turn length is a reciprocal function of the pole-pairs p, however in the single tooth wound machine it is a reciprocal function of the number of stator teeth. This can be written;

$$l_{\text{end}} \propto \begin{cases} k_d\left(\frac{1}{p}\right) ; \text{ Distributed} \\ k_c\left(\frac{1}{Q_s}\right) ; \text{ FSCW} \end{cases} \quad (3)$$

Where Q_s is the number of slots and k_d and k_c are constants. The associated constants, empirically determined, as in equation (3) are such that $k_d > k_c$, and k_c for a double layer winding is smaller than that of a single layer winding. For a machine with concentrated windings, this lowers the copper mass and the stator winding resistance, offsetting the increase in copper mass due to increased fill. The short span, regular coils also have a shorter axial extent. For the same frame size, therefore, the active stator stack length can be increased, further increasing torque density per unit total volume (including case) of the cSynRM.

D. Stator Modularity

As the stator coils in the cSynRM and SRM span only one tooth pitch, it is possible to segment the machine's stator for ease of winding and construction. Large distributed winding machines require a labour intensive and complicated winding procedure. Segmentation of the stator can potentially remove this costly and time consuming manufacturing difficulty. The coils can be wound individually on stator segments and assembled with ease, increasing the manufacturability whilst

aiding to improve the achievable fill factor, of which 60% can readily be achieved. Stator segmentation does however introduce airgaps in the flux path which act to increase the overall airgap in the machine, though this effect will be minimised when the stator is shrink fitted into the case. There has been historic and recent interest in high performance SynRM technology [18-20, 31, 34].

IV. Disadvantages of The Topology

With the associated benefits of FSCW, challenges also arise when applying fractional slot concentrated windings to synchronous reluctance machines. The root cause of these is the high space harmonic content due to the discrete placement of coils around the airgap periphery, which are no longer sinusoidally distributed. Fractional slot concentrated (FSCW), fractional slot distributed (FSDW) and integer slot distributed (ISDW) can be categorised by the number of slots/pole/phase, q, (considering a three phase machine);

$$q = \frac{Q_s}{6p} = \frac{z}{n} = \begin{cases} \text{Fractional} \leq 1, & \text{FSCW} \\ \text{Fractional} > 1, & \text{FSDW} \\ \text{Positive Integer}, & \text{ISDW} \end{cases} \quad (4)$$

Where Q_s, is the number of stator slots and p, is the number of pole pairs. Windings can be both single and double layer (or even higher), the latter of the two reduces the harmonic content due to an increase in the number coils, which are more evenly distributed around the airgap periphery. FSCW can then be split into Grade I and Grade II windings, based upon whether the denominator n, in eq. (4) is even or odd [21]. The grade determines the harmonic ordinates of the winding, dictating the winding factors and MMF harmonic spectra, which are calculated analytically. The applicable harmonics generated by the winding are defined as [22];

$$v = \begin{cases} \pm\frac{1}{n}(6g+2), & n = \text{even} \\ \pm\frac{1}{n}(6g+1), & n = \text{odd} \end{cases} \quad (5)$$

The harmonic subordinate $g = 1,2,3 \ldots$ In machines that have a slot/pole/phase of 0.5 or lower, the main flux path in the air gap region over one rotor pole pitch may consist of one slot and one tooth or less. Thus, the flux distribution can be asymmetrical, manifesting significant space harmonic content which can be even or odd, causing parasitic effects in the machine. Sub-harmonics exist in certain slot-pole combinations (if the numerator, $z \neq 1$), contributing heavily to the iron losses in the machine. As a comparison, the MMF harmonics for an integer slot winding and an equivalent fractional slot concentrated winding are plotted in Fig. 3.

Reduction of these MMF space harmonics may be possible by using a 4 layer winding with tooth-wound [36]. This would imporve the saliency, power factor and torque capability but would increase manufacturing complexity and increase cost. This winding option is not considered further here.

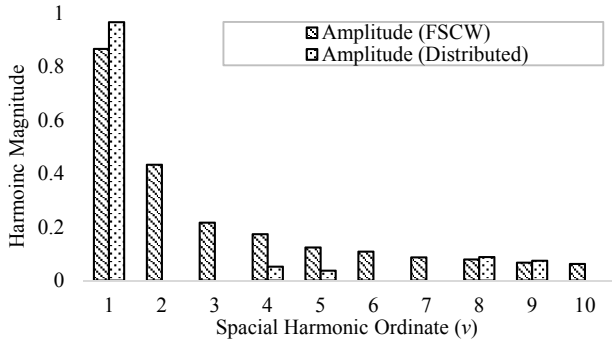

Fig. 3. MMF harmonics of a 36 slot, 4 pole integer slot distributed winding (top) and relative MMF harmonics of a 6 slot, 4 pole fractional slot concentrated winding (bottom) – both are double layer windings.

A. Increased Torque Ripple

Electromagnetic torque is the result of tangential Maxwellian stresses in the airgap of the machine acting upon the rotor. The tangential and radial airgap fields contain harmonics derived from the machine MMF and permeance function space harmonics. These harmonics create parasitic perturbations in the Maxwellian stress, leading to high torque ripple in the cSynRM when compared to a sinusoidally distributed machine [31]. Therefore the torque quality for identical rotors is expected to be lower in the cSynRM. The resultant tangential stress distribution on the rotor surface for field harmonics, v, at a time instant around the airgap periphery, can be expressed [31];

$$\sigma_\theta(\theta) = \frac{1}{\mu_0}\sum_{v=1}^{\infty} B_{\theta v}(\theta) B_{rv}(\theta)\cos(\varphi_{dv}) \quad (6)$$

$B_{\theta v}, B_{rv}$ are the harmonic field magnitudes and φ_d is the angle between the two components. Excessive torque ripple leads to increased acoustic noise and vibration, which is undesirable in many applications, for example military and vehicular applications where low noise and vibration are desirable.

B. Increased Iron Loss

The increased harmonic content in the airgap and the machine magnetic circuit will cause increased eddy and hysteresis losses. These losses will be higher when compared to the iron loss of a conventional synchronous reluctance machine, especially in the surface of the rotor component. Although only transversely laminated rotors are considered in this paper, axially laminated (ALA) type rotors would suffer greater iron loss due to significant eddy currents, causing decreased efficiency and increased rotor heating, however the authors in [35] have went a long way to solving this problem and manufacturability remains the major hindrance to the ALA motor To minimize iron losses, careful consideration of the lamination material and thickness is required, but the degradation in stacking factor where thinner laminations are used must also be taken into account so as to not reduce performance.

C. Decreased Power Factor

The saliency ratio (ξ) of the machine effectively determines the maximum power factor of the machine. This saliency ratio

is derived from d-q axis theory and is defined;

$$\xi = \frac{L_d}{L_q} = \frac{L_{md} + L_{s\sigma}}{L_{mq} + L_{s\sigma}} \quad (7)$$

Where L_d and L_q are the direct and quadrature axis inductances, the stator leakage inductance term $L_{s\sigma}$ and the purely magnetizing components, L_{md} and L_{mq} respectively. For modern synchronous reluctance machines with an axially laminated rotor, saliency ratios of greater than 7 are common [23]. A distributed winding synchronous reluctance machine has a power factor between 0.5 and 0.6 under maximum torque per Ampere. The higher the saliency ratio, the higher the power factor (and efficiency);

$$\cos(\phi)_{\max} = \frac{\xi - 1}{\xi + 1} \quad (8)$$

In the cSynRM, the extra leakage flux increases the stator leakage inductance, effectively reducing the saliency ratio, having a negative impact on the performance of the machine. The limiting value of L_q is in fact $L_{s\sigma}$, so the smaller the *q*-axis magnetizing component the higher leakage has a more pronounced effect.

D. Applicable Slot-Pole Combinations

The *d-q* inductances are of great importance in the synchronous reluctance machine, it is important that L_d is maximised and L_q is minimised. There is however another consideration required, most synchronous reluctance machines in the literature are of $p \leq 2$ type. This is due to a detail in the expressions for the *d-q* magnetizing inductances [22];

$$L_m = \frac{6\tau_p \mu_0 l}{\pi^2 p \delta_{\text{eff}}} (k_{w1} N)^2 \quad (9)$$

δ_{eff} is the effective airgap length and *N* is the number of series turns per phase. Equation (9) shows that the magnetizing inductance is proportional to the reciprocal of the pole pairs for a given rotor pole pitch τ_p. Therefore, for maximum torque production and high power factor a low pole number is required to be selected. In order for concentrated windings to be applicable, $q \leq 0.5$ and thus the available slot pole combinations are presented in Table II [30].

TABLE II
APPLICABLE SLOT-POLE COMBINATIONS (WINDING FACTORS)

	Number of Poles				
Number of Slots	**2**	**4**	**6**	**8**	**10**
3	0.866	0.866	-	0.866	0.866
6	-	0.866		0.866	0.500
9	-	0.617	0.866	0.945	0.945
12	-	-	-	0.866	0.966
15	-	-	-	0.711	0.866

For low pole numbers, the number of slot pole-combinations that allow fractional slot concentrated windings is small. These have fundamental winding factors of maximum 0.866 which is usually considered to be the minimum requirement for consideration of a winding. The lower winding factor will limit the torque capability of the machine, when compared to a machine with a higher fundamental winding factor. It is evident in Table. II that there are more pole-slot combinations for 8 and 10 pole machines, however, the effect of this migration would have an overriding detrimental effect on the magnetizing inductances, power factor and torque capability.

E. Efficiency

FSCW potentially allow for very high efficiency SynRMs (greater than the current IE4 SynRM) or high output machines for traction applications that are simple and low cost to construct. By considering the efficiencies of the cSynRM in relation to a conventional SynRM, the efficiency increase of a cSynRM machine can be expressed (see Appendix A);

$$\Delta\eta = \frac{1}{1 + \frac{J}{K}\left(\frac{1}{\eta_{Dist}} - 1\right)} - \eta_{Dist} \quad (10)$$

Where *J* is a loss ratio and *K* is the shaft power ratio between the two machine types based on conservative estimates of the relative end winding lengths, fundamental winding factors and achievable slot fill factors. Using typical values of these ratios, Figure 4 shows the increase in efficiency by adopting FSCW for the same size machine (4-pole machines with identical stator outer and stack dimensions).

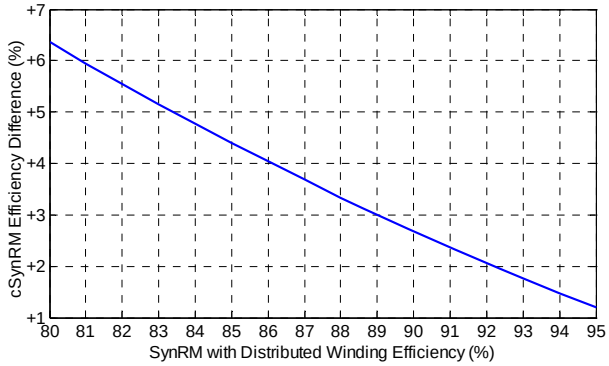

Figure 4: Machine efficiency increase due to shorter end windings and increased fill factor, taking into account lower fundamental winding factors.

This increase in efficiency acts to increase inverter utilization, $\chi = \eta \cdot \cos(\phi)$, however the power factor will be dominant. The torque index is directly dependant on the fundamental winding factor, so a machine with a lower winding factor will have a lower torque producing capability relative to a machine of the same pole number with a higher winding factor. The advantages presented provide a compelling case for the logical transition from distributed to fractional slot concentrated windings.

V. DRIVE AND CONTROL CONSIDERATIONS

In the two main types of reluctance machine, switched and synchronous, the drive topologies are significantly different. The difference is due to the manner in which the machines operate: switched reluctance machines are not rotating field machines, whilst synchronous reluctance machines are. This

allows the synchronous reluctance motor, both the conventional SynRM and the cSynRM, to be supplied by a commercially available voltage source inverter (VSI) (Fig. 5), commonly used with induction machines.

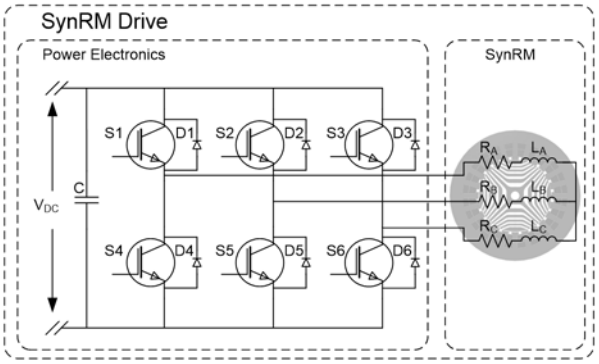

Fig. 5. Synchronous reluctance and induction motor, three-phase voltage source inverter.

The switched reluctance machine however, usually requires an asymmetric half bridge converter [24] (Fig. 6), which are not readily available.

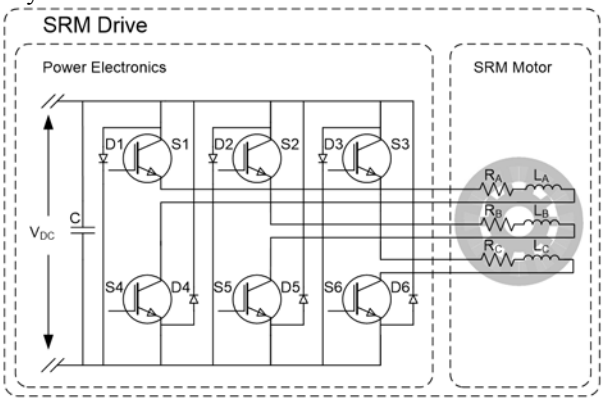

Fig. 6. Switched reluctance motor, three-phase asymmetric half bridge converter.

The asymmetric half bridge converters require a higher number of current sensors and connection leads than the conventional voltage source inverter for the same phase number [24], leading to increased mass and volume. However, recent research has focussed on utilizing conventional VSI technology with higher phase number switched reluctance motors to reduce the number of connections and current sensors [25, 26]. The converter VA requirement of a VSI for synchronous reluctance machines is obviously greater than that for an equivalent size induction machine, due to their lower power factor. It is expected that the converter for a cSynRM is greater again, due to their reduced power factor. This increased VA rating of the converter will inevitably increase its cost. Control of synchronous reluctance machines is achieved in the same manner as that of induction motors, where closed loop vector [27] and direct torque [28] control can be used. A simple shaft encoder can provide position feedback, or sensorless control can be also achieved [29, 34].

Torque ripple is most pronounced in the cSynRM motor-drive due to the contribution of space harmonics to the torque waveform. This could potentially lead to lower speed control precision, though Direct Torque Control (DTC), as the latest ABB drives for the SynRM, can go some way to solving this.

VI. Comparison Motors

As an indication of the level of performance that can be achieved by applying fractional slot concentrated windings to synchronous reluctance motors, three machines based on experimental prototypes are compared. The machine specifications are outlined in Table III.

TABLE III
Machine Specifications

Parameter	*IM*	*SynRM*	*cSynRM*
DC Link Voltage [V]	590	590	590
Winding Factor	0.96	0.96	0.86
Stator Coil Turns	94	94	52
Winding Connection			
Phase Resistance [Ω]	5.1	5.1	0.38
Measured End Winding Axial Extent [mm]	38	38	18.5
Rotor Inertia [kg·m²]	0.00865	0.00616	0.00308

A. Base Comparison Motors

The base comparison machines are a 4-pole commercially available induction motor and a corresponding synchronous reluctance rotor (FEA simulated). Fig. 7 shows cross-sections (FE models) of the two machines.

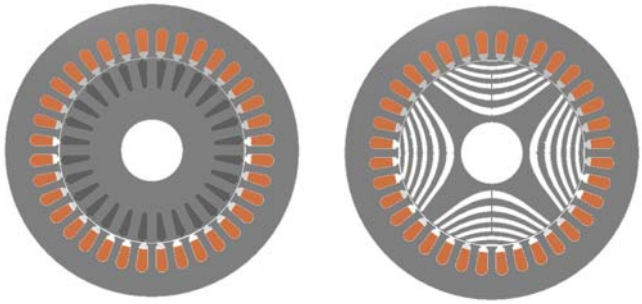

Fig. 7. 36 slot, 24 rotor bar, 4 pole induction motor (left) and corresponding synchronous reluctance motor (right)

B. Novel cSynRM Motor

A fractional slot concentrated winding synchronous reluctance motor (Fig. 8) was designed previously [32] and is compared through finite element to the baseline machines – the magnetic circuit is verified through experimental testing.

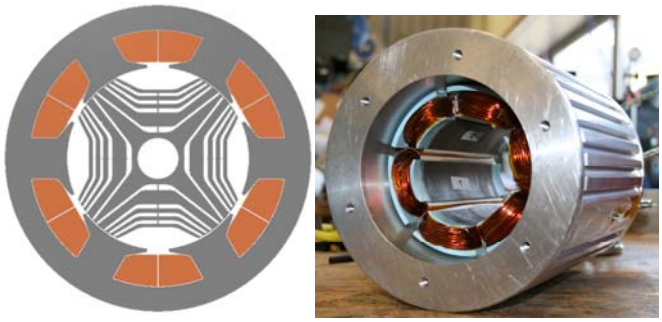

Fig. 8. 6 slot, 4 pole cSynRM. Electromagnetic model (left) and actual motor, end cap and rotor removed, with main dimensions (right)

VII. Machine Comparison

In this comparison, end winding losses based on measured conductor lengths of prototype machines are taken into account. All machines are operated at an identical synchronous speed of 1500rpm, excited with three phase balanced currents containing no-time harmonics. Finite element studies are conducted with Infolytica MagNet.

A. Geometry Considerations

Table IV shows the difference in geometrical parameters for the compared machines (calculated).

TABLE IV
Machine Volumes and Masses

Parameter	*IM*	*SynRM*	*cSynRM*
Stator OD [mm]	155		150
Stack length [mm]	155		150
Electromagnetic Volume [mm^2]	2.92×10^6		2.65×10^6
Rotor core mass (kg)	6.04	4.73	3.39
Rotor bar mass (kg)	0.64	-	-
Rotor end ring mass (kg)	0.12	-	-
Stator core mass (kg)	9.86	9.86	8.88
Stator winding mass (kg)	2.48	2.48	2.05
Total Mass (kg)	19.14	17.07	14.32

Evidently, the mass of the cSynRM is reduced compared to both the IM and SynRM due to a lack of rotor conductors, the rotor design and shorter end windings (as due in part to its lower volume). Thus, the cSynRM has an advantage in not only mass over the two base machines, but raw material cost also, based on a reduced copper mass as the lower rotor mass only contributes to scrap lamination material with no value. The torque per unit volume of the machines is low for traction applications, however, traction applications require greater power machines resulting larger physical size and with significant cooling, which act to increase the torque/power density. The total slot areas per phase are 950 and 1050 mm^2 for the induction motor and the cSynRM prototype respectively. The increase in slot area is attributed to the smaller corner radii in the slot geometry.

B. Constant Loss

The motors are now considered at a constant loss condition of 340W, again driven at their rated speed (or slip). The synchronous speed for all three machines is 1500rpm at 50Hz (4-pole motors), a slot fill factor of 33.8% is used as determined by examining the industrial induction motor. All machines are operated under maximum torque per Ampere control for a fair comparison and saturation effects are also taken into account. Table V shows the motor performances at the rated operating point.

The induction motor is not a cold rotor machine – Joule losses in the rotor reduce the motors efficiency and this is reflected in the comparison. The induction motor exhibits the lowest efficiency, however due to the reduced fundamental winding factor (reduction of approx. 10%) the cSynRM efficiency suffers slightly against the conventional reluctance motor, however it must be noted that this motor is slightly smaller than the other motors.

TABLE V
Machine Comparison (Constant Loss of 340W)

Parameter	*IM*	*SynRM*	*cSynRM*
Loss - Stator Winding (W)	199	287	294
Loss - Rotor cage (W)	128	-	-
Loss - Iron (W)	16.9	56	47
Total Loss (W)	345	343	341
Speed (rpm)	1420	1500	1500
Slip (%)	5.3	-	-
Line Current (A rms)	6.25	7.5	16
Torque (Nm)	15.4	20.1	16.1
Power (kW)	2.29	3.23	2.53
Power Factor	0.80	0.62	0.483
Efficiency	86.8	90.4	88.4
Slot Fill Factor (%)	33.8	33.8	33.8
Current Density (A/mm^2)	6.38	7.66	8.26

Iron losses are increased in the cSynRM, as expected, due to the increased harmonic fluxes in the motor magnetic circuit. As indicated in Section IV – *A*, the torque ripple for the cSynRM is increased over that of the SynRM due to airgap space harmonics, which also reflect the power factors. The induction machine has a high power factor of 0.85 whereas the reluctance motors have reduced power factors, the cSynRM having a power factor of only 0.48. This low power factor impacts the electric drive sizing and also its cost. The power output in the cSynRM is lower than that of the SynRM due to the lower fundamental winding factor and smaller machine size. The machine performance is comparable to that of similar sized switched reluctance motors [33] but is driven from a conventional electric drive system.

C. Increased Fill Factor

In the prototype cSynRM motor, a slot fill factor of 58% was achieved in practice through stator segmentation and winding of a single segment, illustrated in Fig. 9. This decreases the copper loss in the machine and acts to increase efficiency.

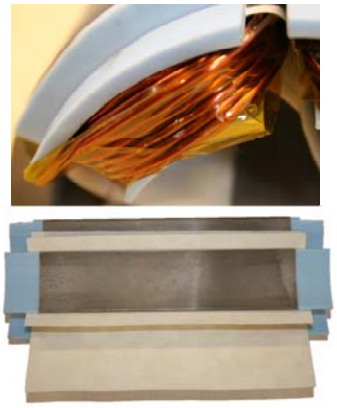

Fig. 9. Upper - End winding of a single tooth coil with a high fill factor – 58% slot fill was achieved. Lower – Single unwound stator segment.

Table VI shows the consequences of increasing the fill factor to levels that are practicable (normalised to 30% fill factor).

TABLE VI
CSYNRM – INCREASED FILL FACTOR

	Parameter					
Fill Factor	Torque (Nm)	Power Factor	Eff (%)	Total Mass (kg)	λ (p.u.)	Estimated Winding Temp (deg C)
0.34 *(Ind)*	16.1	0.482	88.4	15.77	1.11	260
0.50	20.9	0.480	90.7	16.94	1.6	180
0.58 *(Exp)*	23.7	0.477	91.6	17.44	2.09	140
0.70	25.8	0.474	92.3	18.17	3.05	100

For a constant total (consisting of both copper and iron loss) loss of 340W, it is evident from Table VI that the torque density of the cSynRM can be significantly increased by increasing the fill factor: this fill factor must be in the bounds of practical winding. An increase in fill factor from 34% to 58% (the increase in fill factor from the industrial motor to the prototyped motor) provides approximately a 47% increase in torque density and over a 3.62% increase in efficiency. The slot thermal conductivity increases almost four-fold, so the machine with higher fill factor will run cooler than a low fill factor machine. These performance benefits are accompanied by a small 1.66% reduction in power factor and a 15.22% increase in machine weight, which are undesirable. The winding mass increases by 1.67kg in going from 0.34 to 0.58 fill factor which the copper has a market value of only $15 as of March 2014. The corresponding power increase is 1.2kW, leading to an 80W/$ increase in power density by increasing the fill factor. Despite this, the active weight of the cSynRM is still less than the original induction motor.

The power factor decreases due to the increase in stator MMF, creating higher magnitude harmonic fluxes, contributing to an increase in stator leakage inductance. It is unlikely that unless compressed coils are used, a fill factor of 70% will be achieved in practice and a more reasonable value, as achieved in the prototype machine, is around 58%. When increasing the fill factor in order to increase the torque density of the cSynRM, it is important to note that the increase in stator current has an upper limit, even for constant winding copper loss. The increased stator MMF will also increase the magnetic operating point, leading to higher iron loss and saturation. This saturation affects the magnetizing inductance and fundamentally limits the torque capability of a given geometry. The converter needs to be taken into account also, with device selection and cooling becoming an issue at higher current levels.

The estimated winding temperature in Table VI is based upon the measured winding temperature of the prototype motor (see Fig. 13) and then scaled according to the calculated thermal conductivity, λ, as in Eq. 2.

D. *Prototype Verification of FEA Model*

In order to verify the cSynRM machine electromagnetic model used in the comparison, the direct and quadrature axis inductances are measured experimentally. The *direct flux linkage method* is used to determine the *d-q* axis flux linkage curves, based on numerical solution of the following equation;

$$\psi_{d,q}[t] = \int_0^t v_{d,q}[t] - R_s i_{d,q}[t] dt \qquad (11)$$

Where the step DC voltage $v_{d,q}(t)$ causes the current $i_{d,q}(t)$ in the axis (d or q) selected by the rotor position in a rotary table. The experimental apparent inductances, as shown in Fig. 10, are compared with 2D finite element calculations with a lumped end winding inductance of 130μH.

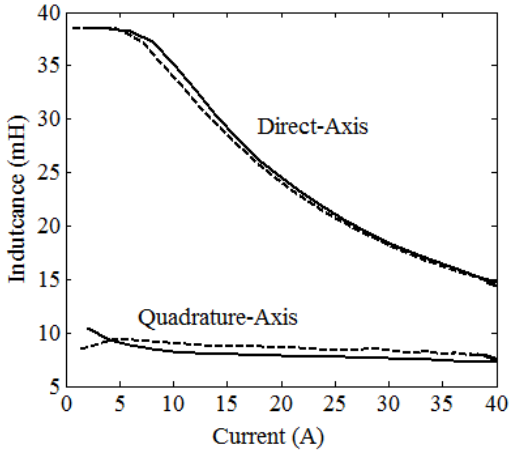

Fig. 10. Experimental (dashed) and finite element (solid) *dq*-axis

The curves in the *d*-axis show a very close match and the *q*-axis inductance shows a lower degree of agreement due to parasitic end effects not considered by the lumped leakage inductance. Experimental results however show that the finite element model will accurately predict machine performance. Figure 11 shows the prototype rotor used during measurements and Figure 12 shows the experimental setup.

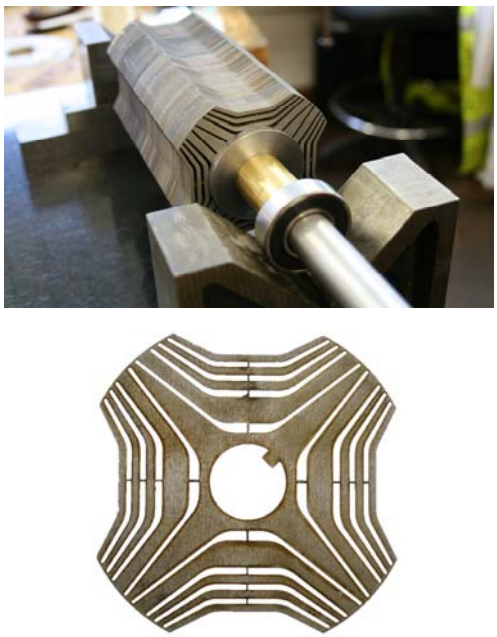

Fig. 11. Prototype rotor lamination stack on the motor shaft before insertion into the stator. Also, the lamination profile is shown.

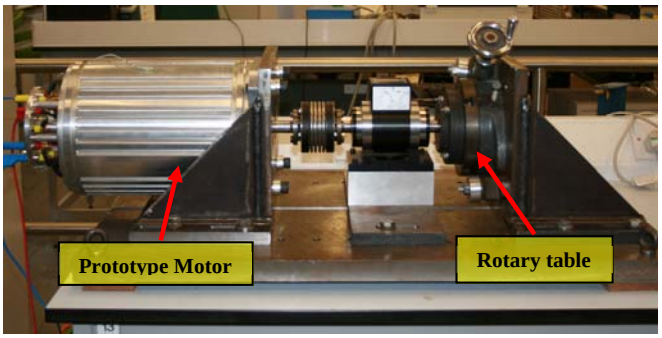

Fig. 12. Static test rig for evaluation of experimental inductance curves.

E. Thermal Measurements and Analysis

The cSynRM prototype is totally enclosed non-ventilated, the slot liner is 0.3mm, with the wire specification at 2mm diameter, grade 2 class F temperature rise insulation. As only static testing is currently being performed, thermal testing was performed by using DC currents to equal 300W of copper loss, representative of the approximate copper loss at rated load. The three phase coils were connected in series during the test and the phase coils have a fill factor of 58%. Figure 13 shows the measured temperature rise of the motor over an 8 hour period with the running induction motor at 100% rated load, the induction motor losses at rated load are 600W and the data stops after one hour due to the hotspot temperature exceeding 140 degrees C at the ambient of 32 deg C.

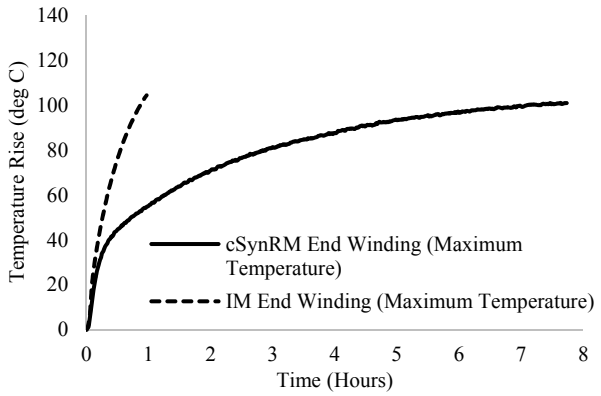

Fig. 13. Experimental temperature rise measurements on the cSynRM with 300W loss and the IM at rated load.

In [37] it is suggested that higher fill factors improve the slot-liner to lamination interface, which acts to decrease the overall thermal resistance of the copper to ambient thermal path. This reference also shows that the slot thermal resistance depends upon the slot areas, surfaces and perimeters. Calculations based on both slot geometries based on the well cited methods in [37,38] indicate the cSynRM has a higher slot thermal resistance if identical fill factors are used, however the improved fill factor reduces the thermal resistance to below that of the induction motor, which coupled with the lower losses (higher efficiency), acts to effect a temperature improvement in the cSynRM over the IM and SynRM.

VIII. Conclusion

This paper presents a first look at the considerations in machine design of a synchronous reluctance machine with fractional slot concentrated windings. The advantages of developing a synchronous reluctance machine with non-overlapping fractional slot concentrated windings are clear. This winding type allows an increase in torque density and efficiency, whilst making the machine easier to construct, with increased robustness and added thermal improvements. The short end windings and stator modularity facilitate these performance increases. Unlike the SRM, the cSynRM can be driven by an off the shelf three phase VSI, but still enjoys the benefits of single tooth coils.

However, the associated challenges in machine design have also been outlined. High MMF space harmonic content impairs performance due to parasitic effects. Torque ripple, low power factor and increased iron loss deserve special consideration when designing a synchronous reluctance machine with fractional slot concentrated windings. The lack of slot-pole combinations available, in conjunction with the low rotor pole number requirement fundamentally limit the topology. A significant increase in torque density can be achieved, along with efficiency and thermal improvements, provided a high fill factor can be achieved, despite the larger slot widths. Poor power factor is a major issue, thus further development is required in order to maximise its potential as an automotive traction motor, or where low cost and robust machines are required for future industrial applications. Finite element models of the cSynRM have been validated by experimental testing of a prototype machine.

Acknowledgment

This work was financially supported in part by Cummins Generator Technologies, Stamford, UK.

Appendix

A. Efficiency Difference - Explanation of Eq. 10

The copper loss in the FSCW machine can be scaled according to;

$$P_{\mathrm{Cu,FSCW}} = P_{\mathrm{Cu,Dist}}\left(\frac{S_{\mathrm{FF,Dist}}}{S_{\mathrm{FF,FSCW}}}\right)\left(\frac{l_{\mathrm{stator,FSCW}} + l_{\mathrm{end,FSCW}}}{l_{\mathrm{stator,Dist}} + l_{\mathrm{lend,Dist}}}\right) = JP_{\mathrm{Cu,Dist}} \quad \text{(A1)}$$

The torque produced by the motor is scaled according to;

$$T_{\mathrm{em,FSCW}} = T_{\mathrm{em,Dist}}\left(\frac{k_{\mathrm{w1,FSCW}}}{k_{\mathrm{w1,Dist}}}\right)^2 = KT_{\mathrm{em,Dist}} \quad \text{(A2)}$$

The factors, K and J are the shaft torque and loss ratios respectively. Working with the machines at identical speed and using the conventional efficiency calculation formula, the resulting equation can be presented in the form of Eq. 7. Typical values are 0.82 and 0.65 for K and J respectively.

B. Staton Slot Thermal Conductivity Expression

In [37] the linear regression fit to the measured slot thermal conductivities of seven induction machines written;

$$\lambda_{\mathrm{eq}} = 0.1076S_{FF} + 0.029967 \quad (B1)$$

This compares well to the slot homogenisation equation, Eq. 2 in the region of $0.25 \leq S_{FF} \leq 0.45$, discrepancies are down to the conductor insulation and any impregnation in the actual machine winding acting to increase the equivalent slot thermal conductivity. The value 0.029967 is air thermal conductivity.

REFERENCES

[1] Kostko, "Polyphase Reaction Synchronous Motor", Journal of AIEE, vol 42, 1923, pp. 1162-1168

[2] Parsa, L..; Toliyat, H.A.; , "Fault-Tolerant Interior-Permanent-Magnet Machines for Hybrid Electric Vehicle Applications," Vehicular Technology, IEEE Transactions on , vol.56, no.4, pp.1546-1552, July 2007

[3] Germishuizen, J.J.; Kamper, M.J.; , "IPM Traction Machine With Single Layer Non-Overlapping Concentrated Windings," Industry Applications, IEEE Transactions on , vol.45, no.4, pp.1387-1394, July-aug. 2009

[4] Pellegrino, G.; Vagati, A.; Guglielmi, P.; Boazzo, B.; , "Performance Comparison Between Surface-Mounted and Interior PM Motor Drives for Electric Vehicle Application," Industrial Electronics, IEEE Transactions on , vol.59, no.2, pp.803-811, Feb. 2012

[5] Pellegrino, G.; Vagati, A.; Boazzo, B.; Guglielmi, P.; , "Comparison of Induction and PM Synchronous motor drives for EV application including design examples," Industry Applications, IEEE Transactions on , vol.PP, no.99, pp.1

[6] Woosuk Sung; Jincheol Shin; Yu-seok Jeong; , "Energy-Efficient and Robust Control for High-Performance Induction Motor Drive With an Application in Electric Vehicles," Vehicular Technology, IEEE Transactions on , vol.61, no.8, pp.3394-3405, Oct. 2012

[7] Niazi, P..; Toliyat, H.A.; Goodarzi, A..; , "Robust Maximum Torque per Ampere (MTPA) Control of PM-Assisted SynRM for Traction Applications," Vehicular Technology, IEEE Transactions on , vol.56, no.4, pp.1538-1545, July 2007

[8] Matsuo, T.; Lipo, T.A.; , "Rotor design optimization of synchronous reluctance machine," Energy Conversion, IEEE Transactions on , vol.9, no.2, pp.359-365, Jun 1994

[9] Moghaddam, Reza R.; Magnussen, F.; Sadarangani, C.; , "Novel rotor design optimization of synchronous reluctance machine for high torque density," Power Electronics, Machines and Drives (PEMD 2012), 6th IET International Conference on , vol., no., pp.1-4, 27-29 March 2012

[10] Brown, Geoff; , "Developing synchronous reluctance motors for variable speed operation," Power Electronics, Machines and Drives (PEMD 2012), 6th IET International Conference on , vol., no., pp.1-6, 27-29 March 2012

[11] EL-Refaie, A.M.; , "Fractional-Slot Concentrated-Windings Synchronous Permanent Magnet Machines: Opportunities and Challenges," Industrial Electronics, IEEE Transactions on , vol.57, no.1, pp.107-121, Jan. 2010

[12] El-Refaie, A.M.; Jahns, T.M.; Novotny, D.W.; , "Analysis of surface permanent magnet machines with fractional-slot concentrated windings," Energy Conversion, IEEE Transactions on , vol.21, no.1, pp. 34- 43, March 2006

[13] Reddy, P.B.; El-Refaie, A.M.; Kum-Kang Huh; Tangudu, J.K.; Jahns, T.M.; , "Comparison of Interior and Surface PM Machines Equipped With Fractional-Slot Concentrated Windings for Hybrid Traction Applications," Energy Conversion, IEEE Transactions on , vol.27, no.3, pp.593-602, Sept. 2012

[14] Abdel-Khalik, A.S.; Ahmed, S.; , "Performance Evaluation of a Five-Phase Modular Winding Induction Machine," Industrial Electronics, IEEE Transactions on , vol.59, no.6, pp.2654-2669, June 2012

[15] Mecrow, B.C.; , "New winding configurations for doubly salient reluctance machines ," Industry Applications, IEEE Transactions on , vol.32, no.6, pp.1348-1356, Nov/Dec 1996

[16] Idoughi, L.; Mininger, X.; Bouillault, F.; Bernard, L.; Hoang, E.; , "Thermal Model With Winding Homogenization and FIT Discretization for Stator Slot," Magnetics, IEEE Transactions on , vol.47, no.12, pp.4822-4826, Dec. 2011

[17] Magnussen, F.; Sadarangani, C.; , "Winding factors and Joule losses of permanent magnet machines with concentrated windings," Electric Machines and Drives Conference, 2003. IEMDC'03. IEEE International , vol.1, no., pp. 333- 339 vol.1, 1-4 June 2003

[18] T. A. Lipo, "Synchronous reluctance machines—A viable alternative for AC drives?", Elect. Mach. Power Syst., vol. 19, pp.659 1991

[19] Vagati, A., "The synchronous reluctance solution: a new alternative in AC drives," Industrial Electronics, Control and Instrumentation, 1994. IECON '94., 20th International Conference on , vol.1, no., pp.1-13 vol.1, 5-9 Sep 1994

[20] Moghaddam, R.R.; Magnussen, F.; Sadarangani, C.; , "Theoretical and Experimental Reevaluation of Synchronous Reluctance Machine," Industrial Electronics, IEEE Transactions on , vol.57, no.1, pp.6-13, Jan. 2010

[21] Salminen, P.; Niemela, M.; Pyhonen, J.; Mantere, J., "Performance analysis of fractional slot wound PM-motors for low speed applications," Industry Applications Conference, 2004. 39th IAS Annual Meeting. Conference Record of the 2004 IEEE , vol.2, no., pp. 1032- 1037 vol.2, 3-7 Oct. 2004

[22] "Design of Rotating Electrical Machines", Juha Pyrhonen, Tapani Jokinen, Valeria Hrabovcova, John Wiley & Sons, 24 Feb 2009

[23] Staton, D.A.; Miller, T.J.E.; Wood, S.E.; , "Maximising the saliency ratio of the synchronous reluctance motor ," Electric Power Applications, IEE Proceedings B , vol.140, no.4, pp.249-259, Jul 1993

[24] "Switched Reluctance Motors and Their Control", T.J.E. Miller, Magna Physics Pub., 1993

[25] Widmer, J. D.; Mecrow, B. C.; Spargo, C. M.; Martin, R.; Celik, T.; , "Use of a 3 phase full bridge converter to drive a 6 phase switched reluctance machine," Power Electronics, Machines and Drives (PEMD 2012), 6th IET International Conference on , vol., no., pp.1-6, 27-29 March 2012 doi: 10.1049/cp.2012.0260

[26] Widmer, J. D.; Martin, R.; Spargo, C. M.; Mecrow, B. C.; Celik, T., "Winding configurations for a six phase switched reluctance machine," *Electrical Machines (ICEM), 2012 XXth International Conference on* , vol., no., pp.532,538, 2-5 Sept. 2012

[27] Boldea, I.; Muntean, N.; Nasar, S.A., "Robust low-cost implementation of vector control for reluctance synchronous machines," *Electric Power Applications, IEE Proceedings* , vol.141, no.1, pp.1,6, Jan. 1994

[28] Bolognani, S.; Peretti, L.; Zigliotto, M., "Online MTPA Control Strategy for DTC Synchronous-Reluctance-Motor Drives," *Power Electronics, IEEE Transactions on* , vol.26, no.1, pp.20,28, Jan. 2011

[29] Ghaderi, A.; Hanamoto, T., "Wide-Speed-Range Sensorless Vector Control of Synchronous Reluctance Motors Based on Extended Programmable Cascaded Low-Pass Filters," *Industrial Electronics, IEEE Transactions on* , vol.58, no.6, pp.2322,2333, June 2011

[30] Emetor Winding Calculator; http://www.emetor.com, 26/03/2012, 8:44am

[31] Kolehmainen, J.; , "Synchronous Reluctance Motor With Form Blocked Rotor," Energy Conversion, IEEE Transactions on , vol.25, no.2, pp.450-456, June 2010

[32] Spargo, C.M.; Mecrow, B.; Widmer, J., "A Semi-Numerical Finite Element Post-Processing Torque Ripple Analysis Technique for Synchronous Electric Machines Utilizing The Airgap Maxwell Stress Tensor," *Magnetics, IEEE Transactions on* , vol.PP, no.99, pp.1,1

[33] Widmer, J.D.; Mecrow, B.C., "Optimized Segmental Rotor Switched Reluctance Machines With a Greater Number of Rotor Segments Than Stator Slots," *Industry Applications, IEEE Transactions on* , vol.49, no.4, pp.1491,1498, July-Aug. 2013

[34] I. Boldea, Reluctance Synchronous Machines and Drives, Oxford University Press (August 1, 1996)

[35] Boldea, I.; Fu, Z. X.; Nasar, S.A., "Performance evaluation of axially-laminated anisotropic (ALA) rotor reluctance synchronous motors," *Industry Applications Society Annual Meeting, 1992., Conference Record of the 1992 IEEE* , vol., no., pp.212,218 vol.1, 4-9 Oct 1992

[36] Fornasiero, E.; Alberti, L.; Bianchi, N.; Bolognani, S., "Considerations on Selecting Fractional-Slot Nonoverlapped Coil Windings," Industry Applications, IEEE Transactions on , vol.49, no.3, pp.1316,1324, May-June 2013

[37] Staton, D.; Boglietti, A.; Cavagnino, A., "Solving the More Difficult Aspects of Electric Motor Thermal Analysis in Small and Medium Size Industrial Induction Motors," *Energy Conversion, IEEE Transactions on* , vol.20, no.3, pp.620,628, Sept. 2005

[38] Boglietti, A.; Cavagnino, A.; Lazzari, M.; Pastorelli, M., "A simplified thermal model for variable-speed self-cooled industrial induction motor," Industry Applications, IEEE Transactions on , vol.39, no.4, pp.945,952, July-Aug. 2003